Journal of Organometallic Chemistry 694 (2009) 466–472

Contents lists available at ScienceDirect

Journal of Organometallic Chemistry

journal homepage: www.elsevier.com/locate/jorganchem

Ferrocene–Mn^{II} π-interaction in the complex $[Fc_2Bpz_2^{Ph}Mn(THF)Cl]$

Linda Kaufmann, Alireza Haghiri Ilkhechi, Hannes Vitze, Michael Bolte, Hans-Wolfram Lerner, Matthias Wagner *

Institut für Anorganische Chemie, Goethe-Universität Frankfurt, Max-von-Laue-Straße 7, D-60438 Frankfurt (Main), Germany

ARTICLE INFO

Article history:
Received 6 October 2008
Received in revised form 7 November 2008
Accepted 14 November 2008
Available online 25 November 2008

Keywords:
Boron
Ligand design
N-Ligands
Manganese
Metallocenes

ABSTRACT

The ferrocene-based bis(pyrazol-1-yl)borate ligands $[Fc_2Bpz_2]^-$ (**[2]**$^-$) and $[Fc_2Bpz_2^{Ph}]^-$ (**[2^{Ph}]**$^-$) have been prepared (Fc: ferrocenyl; pz: pyrazol-1-yl; pz^{Ph}: 3-phenylpyrazol-1-yl). Treatment of **[2]**$^-$ and **[2^{Ph}]**$^-$ with $MnCl_2$ in THF leads to the complexes $[Fc_2Bpz_2Mn(THF)(\mu\text{-}Cl)_2Mn(THF)pz_2BFc_2]$ (**3**) and $[Fc_2Bpz_2^{Ph}Mn(THF)Cl]$ (**3^{Ph}**), respectively, which have been structurally characterized by X-ray crystallography. While there is clearly no ferrocene–Mn^{II} π-coordination in the solid-state structure of **3**, short Mn^{II}–C_5H_4 contacts are established in **3^{Ph}** (shortest Mn–C distances: 2.780(2) Å, 2.872(2) Å). The cyclic voltammograms of **K[2^{Ph}]** and **3^{Ph}** show the first ferrocene/ferricinium redox wave of **3^{Ph}** to be shifted anodically by 0.60 V compared with the first Fe^{II}/Fe^{III} transition of **K[2^{Ph}]**.

1. Introduction

The structural motif of a multiple-decker sandwich complex is ideally suited to bring about electronic communication between the constituent metal ions. This has been impressively demonstrated by Siebert et al. who prepared an organometallic semiconductor based on an extended columnar structure consisting of Ni ions and η^5,μ-2,3-dihydro-1,3-diborolyl ligands [1–3]. For practical reasons, it would, however, be desirable to substitute simple cyclopentadienyl ligands for the sophisticated boron heterocycle. Numerous triple-decker sandwich complexes of the permethylated cyclopentadienyl derivative $[C_5Me_5]^-$ have already been isolated and structurally characterized [4]. In contrast, the number of known examples featuring exclusively the unsubstituted $[C_5H_5]^-$ ligand is still rather small (e.g. $[Ni_2(C_5H_5)_3]^+$ [5], $[Tl_2(C_5H_5)_3]^-$ [6]).

Research in our group is focused on heterobimetallic multiple-decker sandwich complexes consisting of ferrocene and bridging metal ions M^{n+} (**A**; Fig. 1). Oligonuclear as well as polymeric species **A** are known in which M^{n+} is an alkali metal ion [7–14]. Multiple-decker complexes of ferrocene have also been obtained with the group III metal ions Ga^+ and Tl^+ [15–17]. Two structurally characterized **A**-type complexes with M^{n+} being a transition metal ion are the polymeric Ag-complex **B** [18] and the Zn-complex **C** [19] (Fig. 1).

From these examples it becomes evident that chances to observe ferrocene–metal π-interactions are highest when donor solvents can be avoided during complex synthesis. Moreover, if the sandwich complex bears a positive charge, weakly coordinating counteranions are to be selected. In the case of the transition metal species **B** and **C**, the π-interactions are supported by chelating sidearms stabilizing the desired multiple-decker sandwich structure.

The purpose of this paper is to report on a novel class of ferrocene-based ligands that have been specifically designed to maximize the chance for ferrocene–metal π-coordination. As a proof-of-principle, the synthesis and structural characterization of the first ferrocene–Mn^{II} multiple-decker sandwich complex will be presented.

2. Results and discussion

For a more general approach to ferrocene-containing multiple-decker sandwich complexes it is necessary to have the option to use transition metal salts that require strongly coordinating solvents as reaction media. Moreover, we want to establish multiple-decker sandwich motifs not only in the solid state but also in solution. Given this background, the design of ferrocene ligands **K[2]** and **K[2^{Ph}]** (Scheme 1) is based on the following considerations: (i) similar to **B** and **C**, a chelating sidearm should be present, (ii) bis(pyrazol-1-yl)borates are a good choice as supporting ligands, because they offer *two* donor sites and, in addition, attract the metal cation electrostatically, and (iii) the incorporation of two ferrocenyl moieties in the ligand molecule will increase the

* Corresponding author. Fax: +49 69 798 29260.
E-mail address: Matthias.Wagner@chemie.uni-frankfurt.de (M. Wagner).

0022-328X/$ - see front matter © 2008 Elsevier B.V. All rights reserved.
doi:10.1016/j.jorganchem.2008.11.034

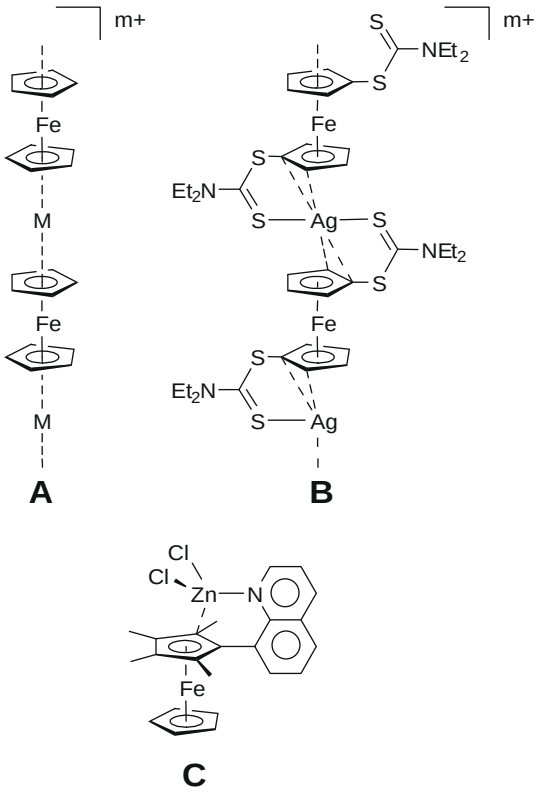

Fig. 1. General structure of a ferrocene-based heterodinuclear multiple-decker sandwich complex **A**; representation of the **A**-type silver complex **B** and of a related zinc complex **C**.

number of conformations that have the potential to bring about ferrocene–metal π-coordination.

2.1. Synthesis and spectroscopical characterization

The ligands **K[2]** and **K[2^{Ph}]** (Scheme 1) were synthesized by treatment of the aminoborane **1**[12] in THF with a mixture of Hpz/Kpz and Hpz^{Ph}/Kpz^{Ph}, respectively (Hpz: pyrazole; Hpz^{Ph}: 3-phenylpyrazole). Heating at reflux temperature for several hours is required to drive the transamination reaction to completion.

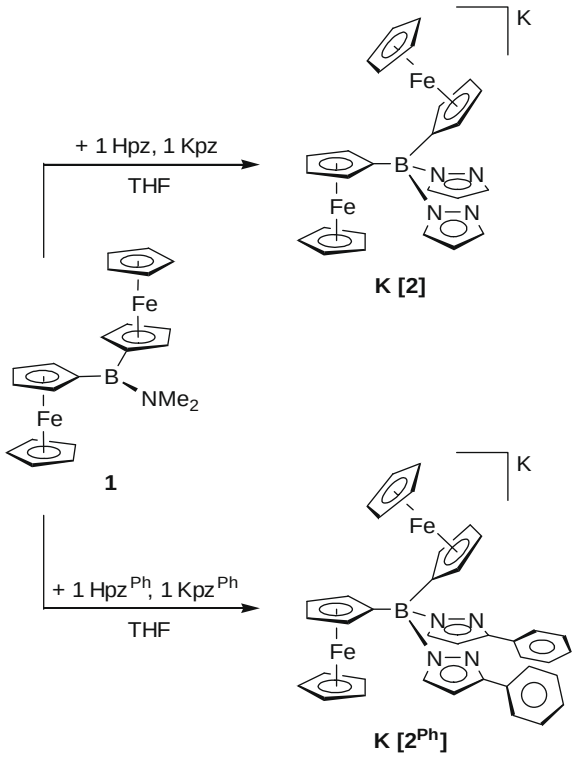

Scheme 1. Synthesis of the ferrocenyl-substituted bis(pyrazol-1-yl)borate ligands **K[2]** and **K[2^{Ph}]**.

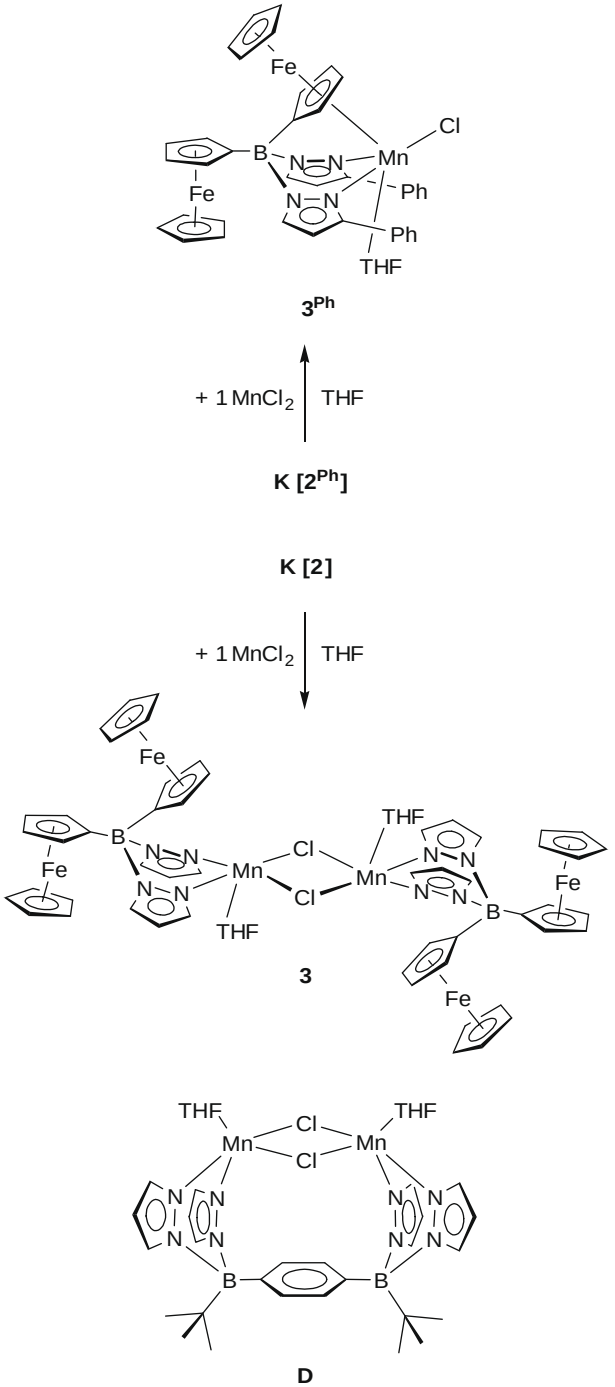

Scheme 2. Synthesis of the Mn^{II} complexes **3** and **3^{Ph}** of the ligands **[2]**$^{-}$ and **[2^{Ph}]**$^{-}$; representation of compound **D** used for comparison.

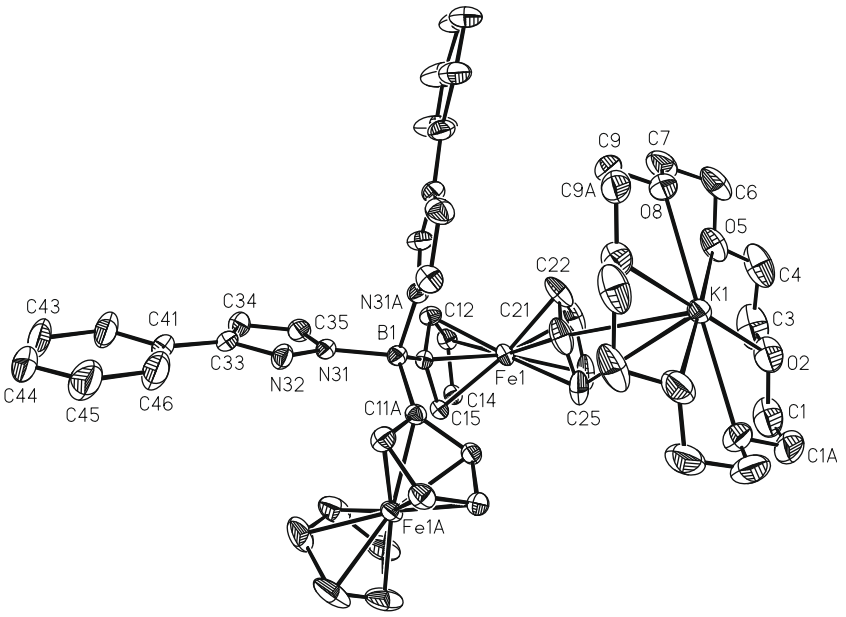

Fig. 2. Structure of **K[2^{Ph}]** (18-crown-6) in the crystal. Displacement ellipsoids are drawn at the 30% probability level. H atoms and the non-coordinating THF molecule are omitted for clarity. Selected bond lengths (Å), bond angles (°), and torsion angles (°): K(1)–C(21) = 3.148(2), K(1)–C(25) = 3.498(3), B(1)–N(31) = 1.593(3), B(1)–C(11) = 1.628(3); N(31)–B(1)–N(31A) = 104.4(2), N(31)–B(1)–C(11) = 106.8(1), N(31)–B(1)–C(11A) = 111.8(1), C(11)–B(1)–C(11A) = 114.8(3); N(32)–C(33)–C(41)–C(46) = –0.5(4). Symmetry transformation used to generate equivalent atoms: A: $-x+1, y, -z+3/2$.

Reaction of **K[2]** or **K[2^{Ph}]** with 1 equiv. of $MnCl_2$ in THF led to the formation of the dimeric complex **3** and the monomeric compound **3^{Ph}**, respectively (Scheme 2).

NMR-spectroscopic data and X-ray structure parameters of **K[2]** have been published elsewhere [12]. The ^{11}B NMR spectrum of **K[2^{Ph}]** shows one resonance at 1.0 ppm, testifying to the presence of tetra-coordinated boron nuclei [20]. The integral values of the phenylpyrazolyl protons on one hand and the ferrocenyl protons on the other are in accord with the proposed 1:1 ratio of these substituents. We observe only one set of signals for the two phenylpyrazolyl rings (the same is true for the two ferrocenyl units) which rules out the possibility that isomers containing one 3-phenylpyrazolyl- and one 5-phenylpyrazolyl donor have been formed. The chemical shift values in the ^{1}H as well as the ^{13}C NMR spectrum of **K[2^{Ph}]** are unexceptional and therefore do not merit further discussion.

The Mn^{II}-ions of **3** and **3^{Ph}** are in their paramagnetic high-spin state. Thus, interpretable NMR spectra were not obtained.

2.2. X-ray crystal structure determinations

K[2^{Ph}] crystallizes from THF/pentane/18-crown-6 as crown ether adduct **K[2^{Ph}]** (18-crown-6) (Fig. 2); the crystal lattice contains 1 equiv. of non-coordinating THF.

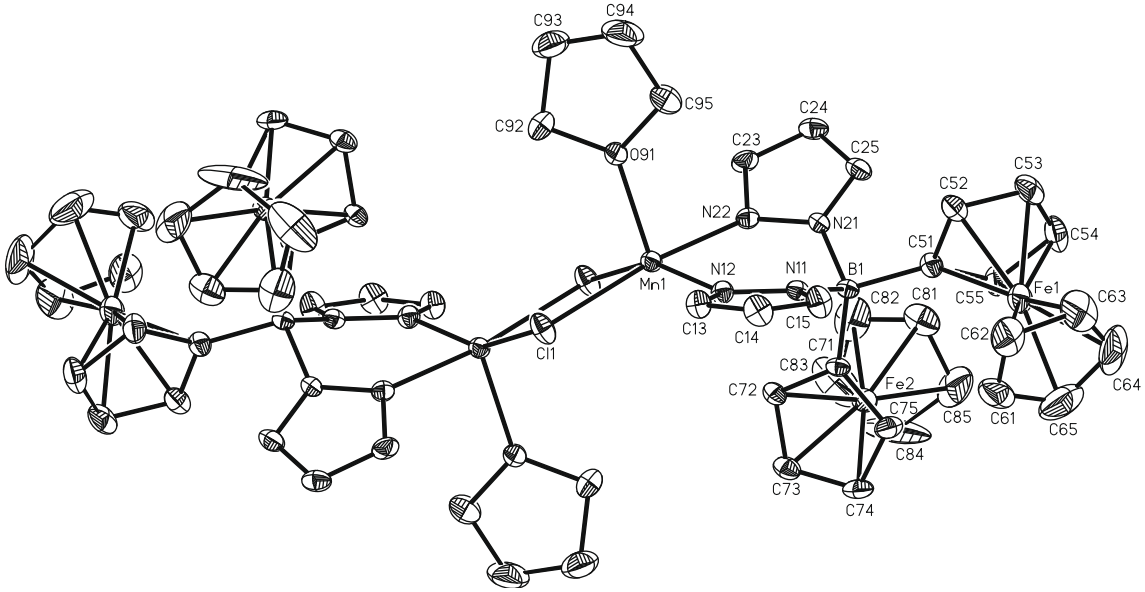

Fig. 3. Structure of **3** in the crystal. Displacement ellipsoids are drawn at the 30% probability level. H atoms are omitted for clarity. Selected bond lengths (Å), bond angles (°), and dihedral angles (°): Mn(1)–Cl(1) = 2.525(1), Mn(1)–Cl(1A) = 2.481(1), Mn(1)–N(12) = 2.139(4), Mn(1)–N(22) = 2.159(4), Mn(1)–O(91) = 2.148(4); Cl(1)–Mn(1)–Cl(1A) = 85.4(1), Mn(1)–Cl(1)–Mn(1A) = 94.6(1), N(12)–Mn(1)–N(22) = 87.7(1); O(91)Mn(1)B(1)//Cp(C(71)) = 16.0. Symmetry transformation used to generate equivalent atoms: A: $-x+1, -y+1, -z+2$.

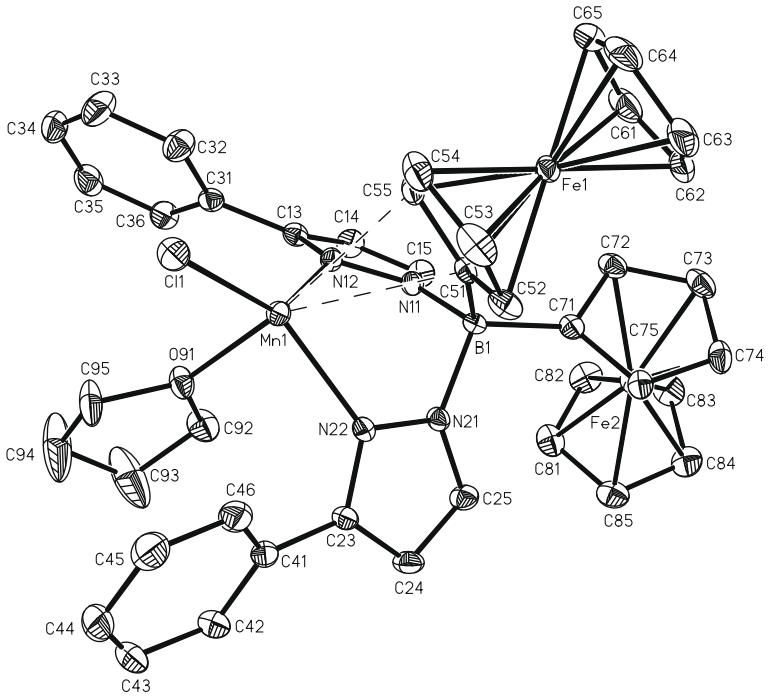

Fig. 4. Structure of $\mathbf{3^{Ph}}$ in the crystal. Displacement ellipsoids are drawn at the 50% probability level. H atoms are omitted for clarity. Selected bond lengths (Å), bond angles (°), and dihedral angles (°): Mn(1)–Cl(1) = 2.316(1), Mn(1)–O(91) = 2.195(1), Mn(1)–N(12) = 2.169(2), Mn(1)–N(22) = 2.152(2), Mn(1)–C(51) = 2.872(2), Mn(1)–C(55) = 2.780(2), Mn(1)–COG(Cp(C(51))) = 3.172; Cl(1)–Mn(1)–O(91) = 96.3(1), Cl(1)–Mn(1)–N(12) = 131.9(1), Cl(1)–Mn(1)–N(22) = 132.6(1), O(91)–Mn(1)–N(12) = 89.7(1), O(91)–Mn(1)–N(22) = 90.5(1), N(12)–Mn(1)–N(22) = 94.9(1); O(91)Mn(1)B(1)//Cp(C(51)) = 66.9. COG: centroid of the cyclopentadienyl ring.

In the solid state, the molecule is located on a C_2-axis running through the boron atom and the potassium ion. Both heterocyclic substituents are bonded in the 3-phenylpyrazol-1-yl form. Each K^+-ion is coordinated by one 18-crown-6 molecule in an equatorial plane. The axial positions are occupied by the carbon atom C(21) of one ferrocene moiety and the carbon atom C(21B) of a second $\mathbf{[2^{Ph}]^-}$ ligand (symmetry transformation used to generate equivalent atoms: B: $-x+2, y, -z+3/2$). The corresponding bond length (K(1)–C(21) = 3.148(2) Å) is close to the sum (3.03 Å [11]) of the ionic radius of K^+ and the half-thickness of an arene ring. Interestingly, the 3-phenylpyrazol-1-yl units are not involved in K^+-coordination at all.

The manganese complex **3** crystallizes as centrosymmetric chloro-bridged dimer (Fig. 3).

Each Mn^{II}-center is chelated by one bis(pyrazol-1-yl)borate ligand (Mn(1)–N(12) = 2.139(4) Å, Mn(1)–N(22) = 2.159(4) Å) and further bonded to two chloride ions (Mn(1)–Cl(1) = 2.525(1) Å, Mn(1)–Cl(1A) = 2.481(1) Å) and one THF molecule (Mn(1)–O(91) = 2.148(4) Å). The resulting coordination polyhedron is closer to a square pyramid than to a trigonal bipyramid (trigonality index τ [21] = 0.29). The ligand environment of the central Mn_2Cl_2 core is reminiscent of the recently published macrocycle **D** [22] (Scheme 2), apart from the fact that **D** contains a bridging ditopic bis(pyrazol-1-yl)borate ligand which enforces a *cis*-arrangement of the two THF ligands. The most important feature of the solid-state structure of **3** is the absence of Mn^{II}–ferrocene π-coordination. In fact, the dihedral angle between the O(91)Mn(1)B(1) plane and the Cp(C(71)) plane is only 16.0°, which means that the edge rather than the π-face of this cyclopentadienyl ring is presented to the Mn^{II}-center.

The presence of bulky phenyl substituents at the 3-positions of the pyrazol-1-yl substituents prevents the dimerization of the corresponding Mn^{II}-complex $\mathbf{3^{Ph}}$ and consequently leads to a tetracoordinated metal center (Fig. 4).

Somewhat surprisingly, the smaller coordination number in $\mathbf{3^{Ph}}$ does not lead to a general contraction of the metal–ligand distances with respect to **3**. Probably as a result of steric crowding, the Mn(1)–O(91) bond (2.195(1) Å) is even elongated by 0.047 Å while the mean value of the Mn–N bonds (Mn(1)–N(12) = 2.169(2) Å, Mn(1)–N(22) = 2.152(2) Å) remains roughly the same. Only the Mn–Cl bond is significantly shorter in $\mathbf{3^{Ph}}$ (Mn(1)–Cl(1) = 2.316(1) Å) as compared to **3**, most likely because the chloro ligand is no longer shared between two Mn^{II}-ions. The [*N,N,O,Cl*] coordination environment of $\mathbf{3^{Ph}}$ is best described as trigonal–pyramidal and thus deviates substantially from the tetrahedral geometry expected for a d^5 high-spin Mn^{II}-ion. We attribute this structural peculiarity to the Fe(1)–ferrocene substituent, which pushes the chloro ligand away. In contrast to **3**, the conformation of the complex is such that a cyclopentadienyl ring now presents its π-face to the Mn^{II}-ion, which is the prerequisite for Mn^{II}–ferrocene π-interaction (dihedral angle O(91)Mn(1)B(1)//Cp(C(51)) = 66.9°). The distance between Mn^{II} and the centroid (COG) of Cp(C(51)) amounts to 3.172 Å; the shortest Mn-C contacts are Mn(1)–C(51) = 2.872(2) Å and Mn(1)–C(55) = 2.780(2) Å. We note in this context that the sum of the ionic radius of Mn^{II} (0.80 Å [23]; coordination number 6, high-spin state) and the half-thickness of an arene ring (1.70 Å [11]) has a comparable value of 2.50 Å.

2.3. Electrochemical investigations

The potassium salt $\mathbf{K[2^{Ph}]}$ and the corresponding Mn^{II}-complex $\mathbf{3^{Ph}}$ were investigated by cyclic voltammetry in order to assess to which extent the close proximity of the Mn^{II}-ion influences the Fe^{II}/Fe^{III} transition(s) of the ferrocene moieties.

The cyclic voltammogram of $\mathbf{K[2^{Ph}]}$ reveals two ferrocene-based one-electron redox transitions with potential values of $E_{1/2}$ = −0.50 V (ΔE = 112 mV) and −0.22 V (ΔE = 115 mV; THF, $[NBu_4][PF_6]$, versus FcH/FcH^+; Fig. 5). Both transitions comply with the following criteria for electrochemical reversibility: the current ratios (i_{pc}/i_{pa}) are constantly equal to one, the current functions $i_{pa}/v^{1/2}$ remain constant and the peak-to-peak separations (ΔE) do

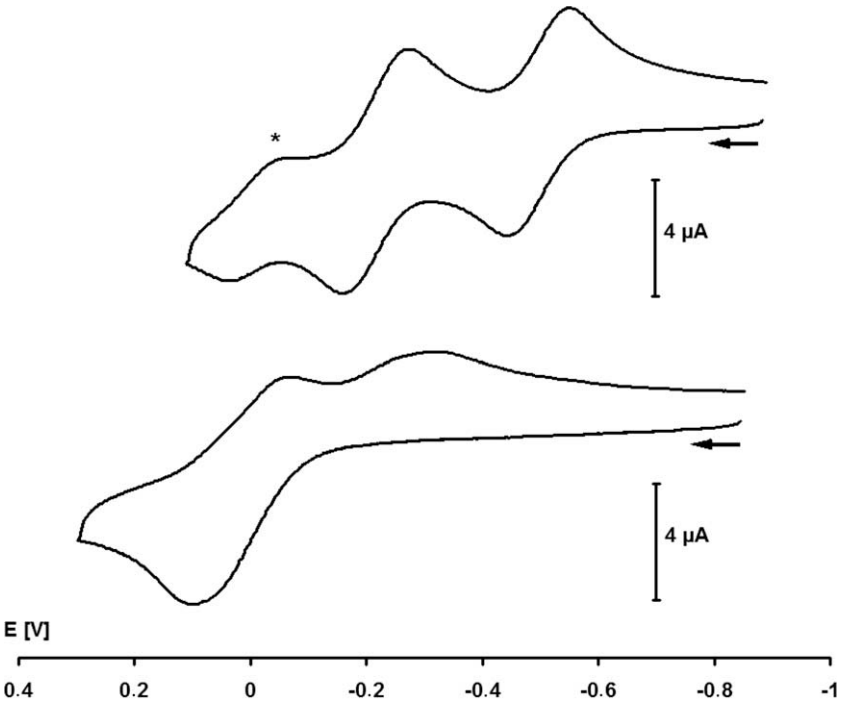

Fig. 5. Cyclic voltammograms of **K[2^{Ph}]** (top) and **3^{Ph}** (bottom) versus FcH/FcH$^+$ (THF, [NBu$_4$][PF$_6$] (0.1 M)); the redox transition of the internal ferrocene standard is marked with an asterisk.

not deviate appreciably from the value found for the internal ferrocene standard (ΔE(FcH); theoretically expected value for a chemically and electrochemically reversible one-electron step: ΔE = 59 mV). The redox potentials of bis(pyrazol-1-yl)borate **K[2^{Ph}]** are anodically shifted with respect to those of the phenyl congener Li[Fc$_2$BPh$_2$] ($E_{1/2}$ = −0.64 V, −0.38 V; CH_2Cl_2, [NBu$_4$][PF$_6$]) [13], likely because of the higher group electronegativity of the pyrazolyl ring compared to the phenyl substituent. The separation between the halfwave potentials, however, which can be regarded as a measure of electronic communication between the two ferrocenyl substituents, is similar in **K[2^{Ph}]** ($\Delta E_{1/2}$ = 0.28 V) and Li[Fc$_2$BPh$_2$] ($\Delta E_{1/2}$ = 0.26 V).

In contrast to **K[2^{Ph}]**, compound **3^{Ph}** features exclusively irreversible redox events (Fig. 5). Starting at a potential value of −0.85 V and taking the sweep into the anodic regime up to a value of 0.30 V, an oxidation wave is observed at E_{pa} = 0.10 V. When the sweep is taken back into the cathodic regime, two irreversible reductions appear with peak potentials at E_{pc} = −0.07 V and −0.32 V. When the oxidative scan is halted at a potential value of −0.10 V, no peak at E_{pc} = −0.32 V can be observed upon re-reduction. Thus, this latter electron transition is related to the product of the anodic redox event at E_{pa} = 0.10 V. Controlled potential coulometric tests performed on THF solutions of **3^{Ph}** (E_w = 0.55 V) yield one electron per molecule. The color of the solution turns to blue-green and the typical absorption of ferricinium derivatives is observed (λ_{max} = 626 nm). Importantly, the cyclic voltammogram of the solution taken prior to the coulometric measurements is identical to the cyclic voltammograms recorded after exhaustive one-electron oxidation and re-reduction.

3. Conclusion

The design of the ferrocenyl-substituted bis(pyrazol-1-yl)borate ligand [Fc$_2$Bpz$_2^{Ph}$]$^-$ (**[2^{Ph}]**$^-$; pz^{Ph}: 3-phenylpyrazol-1-yl) is well-suited to force a transition metal ion into close proximity to the π-face of one of the ferrocenyl cyclopentadienyl rings. This becomes evident from the solid-state structure of the d^5 high-spin Mn^{II}-complex [Fc$_2$Bpz$_2^{Ph}$Mn(THF)Cl] (**3^{Ph}**) which reveals short Mn–C(Cp) contacts even though covalent bonding contributions are probably small due to the half-filled d shell of the Mn^{II}-ion.

Cyclic voltammetric (CV) measurements on the potassium salt **K[2^{Ph}]** show the oxidation of both ferrocenyl moieties to be electrochemically reversible. The more cathodic redox wave of **K[2^{Ph}]** ($E_{1/2}$ = −0.50 V; versus FcH/FcH$^+$) is shifted by 0.60 V into the anodic regime upon formation of the Mn^{II}(THF)Cl-complex **3^{Ph}**. The Mn^{II}-ion apparently remains coordinated to the bis(pyrazol-1-yl)-borate unit even when one ferrocenyl substituent is oxidized, because cyclic voltammograms taken during coulometry never revealed the electrochemical signature of the free ligand **[2^{Ph}]**$^-$.

Multiple-decker sandwich motifs as in **3^{Ph}** are of interest both in materials science (one-dimensional wires) and in homogeneous catalysis (redox-mediated transformations). We are therefore currently working on the synthesis of **3^{Ph}**-type complexes containing metal ions M^{n+} other than Mn^{II} with the aim to maximize the degree of (covalent) ferrocene–M^{n+} π-interaction.

4. Experimental section

4.1. General considerations

All reactions were carried out under a nitrogen atmosphere using Schlenk tube techniques. Solvents were freshly distilled under argon from Na/benzophenone (diethyl ether, THF, d_8-THF) or Na/Pb alloy (pentane, hexane) prior to use. NMR: Bruker AMX 250 and AMX 400. Chemical shifts are referenced to residual solvent peaks (^{1}H, ^{13}C{^{1}H}) or external $BF_3 \cdot Et_2O$ (^{11}B{^{1}H}). Abbreviations: s = singlet, d = doublet, tr = triplet, vtr = virtual triplet, *i* = ipso, *o* = ortho, *m* = meta, *p* = para, pz = pyrazol-1-yl, pz^{Ph} = 3-phenylpyrazol-1-yl. All NMR spectra were run at room temperature. Compounds **1** and **K[2]** were synthesized according to literature procedures [12].

Table 1
Selected crystallographic data for **K[2^{Ph}]** (18-crown-6), **3**, and **3^{Ph}**.

Compound	**K[2^{Ph}]** (18-crown-6)	**3**	**3^{Ph}**
Formula	$C_{50}H_{56}BFe_2KN_4O_6 \times C_4H_8O$	$C_{60}H_{64}B_2Cl_2Fe_4Mn_2N_8O_2$	$C_{42}H_{40}BClFe_2MnN_4O$
Formula weight	1042.70	1354.99	829.68
Color, shape	Orange, plate	Orange, needle	Orange, needle
Temperature (K)	173(2)	173(2)	173(2)
Crystal system	Monoclinic	Triclinic	Triclinic
Space group	*C*2/*c*	$P\bar{1}$	$P\bar{1}$
a (Å)	11.9409(6)	7.7544(8)	9.1061(5)
b (Å)	22.1087(14)	11.5690(15)	14.2802(8)
c (Å)	19.4674(9)	16.9554(19)	16.6423(10)
α (°)	90	92.472(10)	106.772(4)
β (°)	99.308(4)	101.114(9)	101.540(5)
γ (°)	90	98.587(10)	107.936(4)
V (Å^3)	5071.7(5)	1471.8(3)	1869.57(18)
Z	4	1	2
D_{calc} (g cm^{-3})	1.366	1.529	1.474
F(000)	2192	694	854
μ (mm^{-1})	0.710	1.517	1.209
Crystal size (mm^3)	0.42 × 0.37 × 0.20	0.17 × 0.11 × 0.08	0.34 × 0.12 × 0.09
Number of reflections collected	34909	11908	32065
Number of independent reflections (R_{int})	4768 (0.0695)	5423 (0.0761)	6976 (0.0394)
Data/restraints/parameters	4768/0/317	5423/0/361	6976/0/469
GOOF on F^2	1.029	0.970	1.028
R_1, wR_2 ($I > 2\sigma(I)$)	0.0392, 0.0884	0.0564, 0.0971	0.0295, 0.0686
R_1, wR_2 (all data)	0.0549, 0.0936	0.1065, 0.1105	0.0344, 0.0709
Largest difference in peak and hole (e Å^{-3})	0.540 and −0.382	0.545 and −0.483	0.882 and −0.787

4.2. Synthesis of *K[2^{Ph}]*

A suspension of Hpz^{Ph} (0.49 g, 3.39 mmol) and Kpz^{Ph} (0.62 g, 3.39 mmol) in THF (13 mL) was added dropwise with stirring to a solution of **1** (1.44 g, 3.39 mmol) in THF (12 mL) at −78 °C. The reaction mixture was slowly warmed to r.t. and stirred overnight. The resulting orange solution was heated to reflux for 6 h. All volatiles were removed in vacuo and the crude solid product was extracted into diethyl ether (2 × 10 mL). Yield: 2.18 g (91%). X-ray quality crystals of **K[2^{Ph}]**(18-crown-6) were obtained by layering a solution of **K[2^{Ph}]** and 18-crown-6 in THF with pentane via gas-phase diffusion. $^{11}B\{^1H\}$ NMR (128.4 MHz, d_8-THF): δ 1.0 ($h_{1/2}$ = 330 Hz). ^1H NMR (400.1 MHz, d_8-THF): δ 3.76 (s, 10H, C_5H_5), 4.14, 4.64 (2 × vtr, 2 × 4H, $^3J_{HH} = {}^4J_{HH}$ = 1.7 Hz, C_5H_4), 6.45 (d, 2H, $^3J_{HH}$ = 2.0 Hz, pzH-4), 7.13 (tr, 2H, $^3J_{HH}$ = 7.4 Hz, PhH-*p*), 7.29 (vtr, 4H, $^3J_{HH}$ = 7.8 Hz, PhH-*m*), 7.47 (d, 2H, $^3J_{HH}$ = 2.0 Hz, pzH-5), 7.82 (d, 4H, $^3J_{HH}$ = 6.8 Hz, PhH-*o*). $^{13}C\{^1H\}$ NMR (100.6 MHz, d_8-THF): δ 68.8 (C_5H_4), 68.9 (C_5H_5), 75.2 (C_5H_4), 100.3 (pzC-4), 126.1 (PhC-*o*), 127.0 (PhC-*p*), 129.3 (PhC-*m*), 137.4 (pzC-5), 151.3 (PhC-*i*). Elem. Anal. $C_{38}H_{32}BFe_2KN_4$ [706.29]: Calc.: C, 64.62; H, 4.57; N, 7.93; found: C, 64.29; H, 4.79; N, 8.02%.

4.3. Synthesis of *3*

A suspension of **K[2]** · 2 THF (0.027 g, 0.04 mmol) and $MnCl_2$ (0.005 g, 0.04 mmol) in THF (10 mL) was stirred at r.t. for 5 d. After filtration, all volatiles were removed from the filtrate in vacuo and the crude solid product was extracted with hexane (2 × 10 mL). The insoluble solid residue was dissolved in THF. Few single crystals of **3** were obtained by gas-phase diffusion of hexane into this THF solution.

4.4. Synthesis of *3^{Ph}*

A suspension of **K[2^{Ph}]** (0.200 g, 0.28 mmol) and $MnCl_2$ (0.035 g, 0.28 mmol) in THF (20 mL) was stirred at r.t. for 5 d, whereupon a brown solution and a white precipitate formed. The mixture was filtered, all volatiles were removed from the filtrate in vacuo, and the crude solid product was extracted with hexane (2 × 10 mL). Single crystals were grown by gas-phase diffusion of hexane into a THF solution of **3^{Ph}**. Yield: 0.07 g (31%). Elem. Anal. $C_{42}H_{40}BClFe_2MnN_4O$ [829.68]: Calc.: C, 60.80; H, 4.86; N, 6.75; found: C, 60.39; H, 4.65; N, 6.83%.

4.5. X-ray crystallography

Single crystals of **K[2^{Ph}]**(18-crown-6), **3**, and **3^{Ph}** were analyzed using a Stoe IPDS-II two-circle diffractometer with graphite-monochromated Mo Kα radiation. Empirical absorption corrections with the MULABS option [24] in the program PLATON [25] were performed; the minimum and maximum transmissions were 0.7547/0.8710 (**K[2^{Ph}]**(18-crown-6)), 0.7826/0.8883 (**3**), and 0.6839/0.8990 (**3^{Ph}**). Equivalent reflections were averaged. The structures were solved by direct methods [26] and refined with full-matrix least-squares on F^2 using the program SHELXL-97 [27]. Hydrogen atoms were placed on ideal positions and refined with fixed isotropic displacement parameters using a riding model. Compound **K[2^{Ph}]**(18-crown-6) contains 1 equiv. of non-coordinating THF molecules in the crystal lattice. Each of these molecules is disordered about a center of inversion with equal occupancy factors. Selected crystallographic data are compiled in Table 1.

4.6. Electrochemical measurements

All electrochemical measurements were performed using an EG&G Princeton Applied Research 263A potentiostat with a glassy carbon disc working electrode. Carefully dried (Na/benzophenone) and degassed THF was used as the solvent and $[NBu_4][PF_6]$ as the supporting electrolyte (0.1 M). All potential values are referenced against the FcH/FcH^+ couple.

Acknowledgments

Financial funding by the *Fonds der Chemischen Industrie* (FCI) and the *Deutsche Forschungsgemeinschaft* (DFG) is acknowledged. L.K. wishes to thank the "Hessisches Ministerium für Wissenschaft und Kunst" for a Ph.D. grant.

Appendix A. Supplementary material

CCDC 687777 (**K[2^{Ph}]**(18-crown-6)), 687776 (**3**) and 687775 (**3^{Ph}**) contain the supplementary crystallographic data for this paper. Supplementary data associated with this article can be found, in the online version, at doi:10.1016/j.jorganchem.2008.11.034.

References

[1] W. Siebert, Angew. Chem. Int. Ed. 24 (1985) 943–958.
[2] T. Kuhlmann, S. Roth, J. Rozière, W. Siebert, Angew. Chem. Int. Ed. 25 (1986) 105–107.
[3] M.Y. Lavrentiev, H. Köppel, M.C. Böhm, Chem. Phys. 169 (1993) 85–102.
[4] N.J. Long, Metallocenes, Blackwell Science, London, 1998.
[5] A. Salzer, H. Werner, Angew. Chem. Int. Ed. 11 (1972) 930–932.
[6] D.R. Armstrong, A.J. Edwards, D. Moncrieff, M.A. Paver, P.R. Raithby, M.-A. Rennie, C.A. Russell, D.S. Wright, Chem. Commun. (1995) 927–928.
[7] W. Clegg, K.W. Henderson, A.R. Kennedy, R.E. Mulvey, C.T. O'Hara, R.B. Rowlings, D.M. Tooke, Angew. Chem., Int. Ed. 40 (2001) 3902–3905.
[8] P.C. Andrikopoulos, D.R. Armstrong, W. Clegg, C.J. Gilfillan, E. Hevia, A.R. Kennedy, R.E. Mulvey, C.T. O'Hara, J.A. Parkinson, D.M. Tooke, J. Am. Chem. Soc. 126 (2004) 11612–11620.
[9] A. Haghiri Ilkhechi, M. Scheibitz, M. Bolte, H.-W. Lerner, M. Wagner, Polyhedron 23 (2004) 2597–2604.
[10] G.W. Honeyman, A.R. Kennedy, R.E. Mulvey, D.C. Sherrington, Organometallics 23 (2004) 1197–1199.
[11] A. Haghiri Ilkhechi, J.M. Mercero, I. Silanes, M. Bolte, M. Scheibitz, H.-W. Lerner, J.M. Ugalde, M. Wagner, J. Am. Chem. Soc. 127 (2005) 10656–10666.
[12] A. Haghiri Ilkhechi, M. Bolte, H.-W. Lerner, M. Wagner, J. Organomet. Chem. 690 (2005) 1971–1977.
[13] L. Kaufmann, H. Vitze, M. Bolte, H.-W. Lerner, M. Wagner, Organometallics 26 (2007) 1771–1776.
[14] J.J. Morris, B.C. Noll, G.W. Honeyman, C.T. O'Hara, A.R. Kennedy, R.E. Mulvey, K.W. Henderson, Chem. Eur. J. 13 (2007) 4418–4432.
[15] S. Scholz, J.C. Green, H.-W. Lerner, M. Bolte, M. Wagner, Chem. Commun. (2002) 36–37.
[16] Y. Sarazin, D.L. Hughes, N. Kaltsoyannis, J.A. Wright, M. Bochmann, J. Am. Chem. Soc. 129 (2007) 881–894.
[17] Y. Sarazin, N. Kaltsoyannis, J.A. Wright, M. Bochmann, Organometallics 26 (2007) 1811–1815.
[18] O. Crespo, M.C. Gimeno, P.G. Jones, A. Laguna, C. Sarroca, Chem. Commun. (1998) 1481–1482.
[19] M. Enders, G. Ludwig, H. Pritzkow, Organometallics 21 (2002) 3856–3859.
[20] H. Nöth, B. Wrackmeyer, Nuclear magnetic resonance spectroscopy of boron compounds, in: P. Diehl, E. Fluck, R. Kosfeld (Eds.), NMR Basic Principles and Progress, Springer, Berlin, 1978.
[21] For five-coordinate complexes, the parameter $\tau = (\theta - \varphi)/60^\circ$ provides a quantitative measure of whether the ligand sphere more closely approaches a square–pyramidal ($\tau = 0$) or a trigonal-bipyramidal geometry ($\tau = 1$; θ, φ are the two largest bond angles and $\theta \geqslant \varphi$), cf. A.W. Addison, T. N. Rao, J. Reedijk, J. van Rijn, G.C. Verschoor, J. Chem. Soc., Dalton Trans. (1984) 1349–1356.
[22] S. Bieller, M. Bolte, H.-W. Lerner, M. Wagner, Inorg. Chem. 44 (2005) 9489–9496.
[23] A.F. Holleman, N. Wiberg, Lehrbuch der Anorganischen Chemie, 101 ed., de Gruyter, Berlin, New York, 1995.
[24] R.H. Blessing, Acta Crystallogr. A 51 (1995) 33–38.
[25] A.L. Spek, J. Appl. Crystallogr. 36 (2003) 7–13.
[26] G.M. Sheldrick, Acta Crystallogr. A 46 (1990) 467–473.
[27] G.M. Sheldrick, SHELXL-97, A Program for the Refinement of Crystal Structures, Universität Göttingen, 1997.